^{17}O quadrupole coupling and the origin of ferroelectricity in isotopically enriched $BaTiO_3$ and $SrTiO_3$

2008 J. Phys.: Condens. Matter 20 085204

(http://iopscience.iop.org/0953-8984/20/8/085204)

J. Phys.: Condens. Matter **20** (2008) 085204 (6pp) doi:10.1088/0953-8984/20/8/085204

^{17}O quadrupole coupling and the origin of ferroelectricity in isotopically enriched $BaTiO_3$ and $SrTiO_3$

R Blinc[1], V V Laguta[2], B Zalar[1], M Itoh[3] and H Krakauer[4]

[1] J Stefan Institute, Jamova 39, 1000 Ljubljana, Slovenia
[2] Institute of Physics, AS CR, Cukrovarnicka 10, 16253 Prague, Czech Republic
[3] Materials and Structures Laboratory, Tokyo Institute of Technology, 4259 Nagatsuta, Midori, Yokohama 226-8503, Japan
[4] College of William and Mary, Williamsburg, VA, USA

Received 22 October 2007, in final form 5 December 2007
Published 1 February 2008
Online at stacks.iop.org/JPhysCM/20/085204

Abstract
The ^{17}O electric field gradient (EFG) and chemical shift tensors have been determined in the paraelectric and ferroelectric phases of isotopically enriched $BaTiO_3$ and $SrTiO_3$ single crystals via ^{17}O NMR. This is the first determination of the ^{17}O EFG and chemical shift tensors in any oxide perovskite crystal. The difference in the ^{17}O chemical shifts between $BaTiO_3$ and $SrTiO_3$ is relatively small, whereas there is a large difference in the ^{17}O EFG tensors even in the cubic phases. Density functional theory calculations indicate that the difference in the ^{17}O EFGs is due to a crystal cell volume effect together with effects due to the difference in ionic radii of Ba and Sr that result in a larger distortion of the nearly spherical charge distribution around the oxygen in $BaTiO_3$.

$BaTiO_3$ and $SrTiO_3$ are two of the technologically most important and most investigated ferroelectric and dielectric materials [1]. They are also considered to be the classical examples of soft mode type phase transitions [1–3]. Since the discovery of ferroelectricity in $BaTiO_3$ in 1945 and the observation of the antiferrodistortive transition in $SrTiO_3$ [1, 4], there have been many attempts to understand the transition mechanism and the nature of the difference between these two systems from both semiempirical models and first principles [5–10].

These studies have been intensified since a low temperature ferroelectric phase has been discovered [11] in ^{18}O isotopically enriched $SrTiO_3$. The problem of the origin of ferroelectricity in these systems is still open. This is particularly important for the first-principles design of new multiferroic multifunctional ferroelectric systems and integrated ferroelectrics where $BaTiO_3$ and $SrTiO_3$ are model materials. Basic information about the polarizability and bonding of the titanium and oxygen ions in particular is still missing.

Here we report on a determination of ^{17}O quadrupole coupling—respectively electric field gradient (EFG)—and chemical shift tensors in paraelectric and ferroelectric isotopically enriched $BaTiO_3$ and $SrTiO_3$ via ^{17}O single crystal NMR. To the best of our knowledge this is the first determination of ^{17}O electric field gradient and ^{17}O anisotropic chemical shift tensors in any oxide perovskite single crystals. Because EFGs depend only on the nuclear positions and the electronic charge density, they provide a very sensitive local probe of the electronic structure and may throw new light on the origin of ferroelectricity in the systems.

Previous ^{17}O NMR studies in $BaTiO_3$ and $SrTiO_3$ [12, 13] were performed on powder samples that allowed determination of only the isotropic part of the ^{17}O chemical shift. Bastow *et al* [13] tried also to extract data on ^{17}O chemical shift anisotropy in cubic $SrTiO_3$. However, they fitted the NMR lineshape by a non-axial symmetry chemical shift tensor, that does not agree with the pure tetragonal symmetry of the oxygen sites. These two papers also provide upper estimates for the ^{17}O quadrupolar coupling constants based on the analysis of the central band line width. Therefore, in contrast to our single crystal data, they did not resolve the difference in the value of the quadrupole constant between $BaTiO_3$ and $SrTiO_3$ materials. Our single crystal measurements show a large difference between $BaTiO_3$ and $SrTiO_3$ in the electric field gradients and quadrupole coupling at the oxygen sites. The

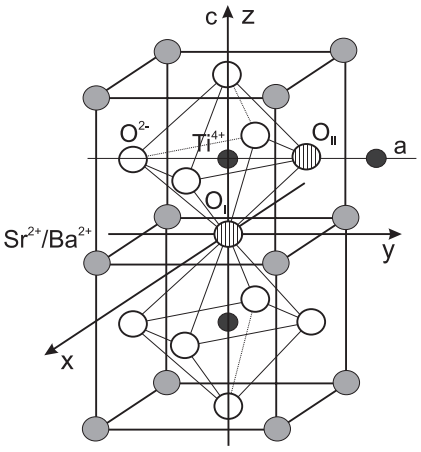

Figure 1. Schematic view of the $SrTiO_3/BaTO_3$ crystal structure showing two sets of structurally non-equivalent oxygen sites O_I and O_{II} in the polar tetragonal phase of $BaTiO_3$.

difference in the ^{17}O chemical shift tensors between these two systems is on the other hand found to be small.

To gain further insight into these results, we have also calculated the electric field gradients, using first-principles density functional theory (DFT), within the local density (LDA [14]) and generalized gradient (GGA/PBE [15]) approximations. The all-electron full-potential linearized augmented plane wave (LAPW) method with the local orbital (LAPW+LO) extension [16] was used. The local orbital extension yields the most accurate treatment of atoms with extended semi-core orbitals. LAPW+LO was used to treat the semi-core Ba(5s, 5p) and Sr(4s, 4p) states variationally along with the valence states. Sphere radii were 2.0 (Ba, Sr), 1.85 (Ti), and 1.7 (O) Bohr, and well converged basis sets were used (cutoff RKMAX = 8.5 [16]). No shape approximations are made within the spheres for the charge density or potential in the method, which is crucial, of course, to obtain accurate electric field gradients. Accurate Brillouin sampling used up to $6 \times 6 \times 6$ k-point grids [17].

At high temperatures $BaTiO_3$ and $SrTiO_3$ have the ideal ABO_3 perovskite centrosymmetric cubic structure [1], $Pm\bar{3}m$. According to the classical model the A ions, i.e. Ba^{2+} and Sr^{2+}, are at the corners and the B, i.e. Ti^{4+}, ions at the center of the unit cell. The oxygens are at the face centers (figure 1). The oxygen site is the only site in the perovskite lattice with a non-cubic point group symmetry. ^{17}O electric quadrupole coupling is therefore allowed by symmetry even in the high temperature cubic phase.

The ^{17}O ($I = 5/2$, natural abundance 0.037%) quadrupole perturbed ^{17}O NMR spectra of a $\sim 10\%$ ^{17}O enriched $BaTiO_3$ single crystal with dimensions $5 \times 3 \times 0.3$ mm^3 and $T_c \approx 403$ K and of a SrTi $[^{16}O_{0.285}\ ^{17}O_{0.43}\ ^{18}O_{0.285}]_3$ single crystal with dimensions $4 \times 3 \times 0.3$ mm^3 and $T_c \approx 12$ K have been measured at a Larmor frequency $\omega_L/2\pi = 51.5177$ MHz corresponding to a magnetic field of $B_0 = 8.92$ T. The isotopic exchange method has been described in [11]. A four phase solid spin-echo sequence was used to observe the ^{17}O central and satellite transitions which spread to a range of ± 0.5 MHz. The length of the $\pi/2$ pulse was typically 1.6–2 μs. The repetition time varied from 15 min at room temperatures to several hours at 10 K due to the extremely long spin–lattice relaxation time of the ^{17}O nuclei. A 10–12 h accumulation of the NMR signal was needed to obtain a sufficient signal-to-noise ratio. The chemical shifts were measured with respect to H_2O.

For each oxygen site we expect $2I = 5$ ^{17}O NMR lines. For the case of axial symmetry of the EFG tensor the position of the $(m - 1 \leftrightarrow m)$ ^{17}O transition relative to $\omega_L/2\pi$ is [18]

$$\nu_m^{(1)} = -\nu_Q(m - 1/2)(3\cos^2\theta - 1)/2. \qquad (1)$$

Here θ is the angle between $\mathbf{B}_0$ and the direction of the largest principal axis of the EFG tensor, $\nu_Q = 3K/[2I(2I-1)]$ is the quadrupole frequency, $K = e^2qQ/h$ is the ^{17}O electric quadrupole constant [18], $eq = V_{ZZ}$ is the largest eigenvalue of the EFG tensor and $eQ = -2.6 \times 10^{-2}e \times 10^{-24}$ cm^2 is the ^{17}O quadrupole moment.

The ^{17}O NMR spectra of $BaTiO_3$ in the paraelectric cubic and the ferroelectric tetragonal and orthorhombic phases [1] are shown in figure 2 for the orientation where $\mathbf{B}_0$ is approximately parallel to the [001] direction and the tilt angle is 8° in the [100] plane.

The presence of satellites shows that the ^{17}O quadrupole coupling is indeed non zero even in the paraelectric cubic phase at 420 K. This is related to the fact that each oxygen ion is surrounded by two Ti ions symmetrically located on the connecting Ti–O–Ti line (figure 1). The actual local symmetry at the oxygen sites in the cubic phase is thus tetragonal. There are three chemically equivalent but physically non-equivalent ^{17}O sites in the unit cell, with the largest principal axes of the EFG tensors parallel to the local tetragonal axes. The local tetragonal axes are oriented along the [100], [010] and [001] directions so that the angle between them is 90°. At the orientation $\mathbf{B}_0 \| \langle 001 \rangle$ the ^{17}O NMR lines from two sites should coincide, whereas the lines of the third site should be displaced and weaker by a factor of two.

The observed ^{17}O NMR spectra of cubic $BaTiO_3$ can indeed be explained by this model. At $\mathbf{B}_0 \| [001]$ all transitions are doublets with an intensity ratio of 2:1. The splitting corresponds to a 90° difference in the orientation of the largest principal axes of the axially symmetric EFG tensors. The distance between $m \leftrightarrow m - 1$ and $-m + 1 \leftrightarrow -m$ satellite transitions is independent of the chemical shifts [14]. The ^{17}O quadrupole frequency obtained from the separation of the satellites is $\nu_Q = 231.9 \pm 0.5$ kHz at 420 K. The asymmetry parameter of the EFG tensor is zero, $\eta = 0$, as indeed expected for local tetragonal symmetry.

In the ferroelectric tetragonal phase below $T_c = 403$ K the ^{17}O NMR spectra of $BaTiO_3$ change significantly (figure 2). In view of the tetragonal distortion of the unit cell— $c/a = 1.014$ at 300 K—the three physically non-equivalent O sites are no longer chemically equivalent. Instead, we have now two sets of chemically non-equivalent ^{17}O sites O_I and $O_{II} \equiv O_{III}$ with different distances from the Ti ions and different quadrupole frequencies: $\nu_{O_I} = 194.0 \pm 0.5$ kHz and $\nu_{O_{II}} = \nu_{O_{III}} = 241.7 \pm 0.5$ kHz at 300 K. O_I corresponds to the oxygen ion in the Ti–O–Ti chain along the polar ferroelectric c-axis whereas O_{II} and O_{III} correspond to the oxygens in the Ti–O–Ti chains along the a and b crystal axes, respectively (figure 1). The

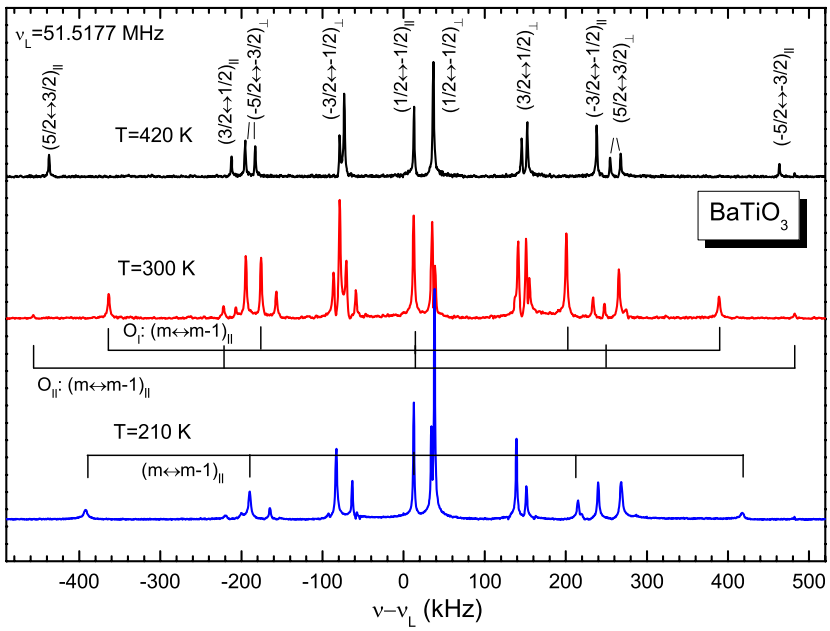

Figure 2. Quadrupole perturbed ^{17}O NMR spectra of ^{17}O enriched $BaTiO_3$ at 420 K (cubic phase), 300 K (tetragonal phase) and 210 K (orthorhombic phase). The indices '$\|$' and '$\perp$' denote that $\mathbf{B}_0$ is parallel or perpendicular to the largest principal axis of the EFG tensor. For tetragonal and orthorhombic phases only $(m \leftrightarrow m-1)_{\|}$ transitions are labeled.

(This figure is in colour only in the electronic version)

Table 1. ^{17}O NMR data in BaTi $^{16}O_{0.9}$ $^{17}O_{0.1}$. Chemical shift values are given relative to H_2O.

Temperature	ν_Q (MHz)	$\lvert V_{zz}\rvert$ (V m^{-2})	δ_{iso} (ppm)	δ_{ax} (ppm)	δ_{iso} [12]	δ_{iso} [13]
420 K: cubic phase	0.2319(5)	2.458×10^{21}	546(5)	−150(1)	—	—
300 K: tetragonal phase	0.2417(5)[a]	2.562×10^{21}	520(5)	−142(1)	530	523
	0.1940(5)[b]	2.056×10^{21}	570(5)	−171(1)	553	564
210 K: orthorhombic phase	0.2086(10)	2.211×10^{21}	—	—	—	—

[a] The largest EFG component is perpendicular to polarization P.
[b] The largest EFG component is parallel to polarization P.

largest principal axis of the EFG tensor is thus parallel to the polarization for O_I and perpendicular to the polarization for $O_{II} \equiv O_{III}$. The EFG tensor at O_I is axially symmetric whereas the one for $O_{II} = O_{III}$ should be rhombic. The deviation from axial symmetry is however too small to be detected.

Knowing the ^{17}O quadrupole coupling, we can determine the ^{17}O chemical shift tensor from the positions of the lines in the ^{17}O NMR spectra. For this, the measured spectra were fitted using a numerical diagonalization of the ^{17}O spin Hamiltonian [19] that allowed us to determine the precise values of the chemical shift tensor components. In the cubic phase of $BaTiO_3$ the isotropic part of the ^{17}O chemical shift tensor relative to water is 546 ppm whereas the uniaxial component, determining the anisotropic part—which is non zero in view of the tetragonal point symmetry of the oxygen sites, is −150 ppm. The corresponding isotropic values in the tetragonal phase at 300 K are $\delta_{iso} = 520$ and 570 ppm, whereas the uniaxial components are $\delta_{ax} = -142$ and −171 ppm for O_{II} and O_I sites, respectively. The isotropic parts of the ^{17}O chemical shift tensors well agree with earlier determinations from magic angle spinning (MAS) ^{17}O NMR [12, 13] (for comparison, see table 1).

In the orthorhombic phase of $BaTiO_3$ the polarization direction changes but the largest principal axis of the ^{17}O EFG tensor is still directed along the Ti–O–Ti chains. The other two principal axes are now pointing in the ⟨110⟩ directions in agreement with the orthorhombic symmetry. The ^{17}O quadrupole frequency is $\nu_Q = 213.2 \pm 0.5$ kHz at 260 K and $\nu_Q = 208.6 \pm 0.5$ kHz at 210 K. The measured ^{17}O NMR spectral data are listed in table 1.

The value of the ^{17}O quadrupole frequency in the orthorhombic phase at 210 K is in reasonable agreement with the value of Singh [20], $V_{zz} = -1.96 \times 10^{21}$ V m^{-2}, calculated for the rhombohedral phase using the LDA. This is not surprising, as in the eight-site model [21, 22] in the orthorhombic phase the ions will be displaced along two different ⟨111⟩ directions, but by amounts similar to those in the rhombohedral phase. Within the eight-site model the EFG values should therefore be similar in the orthorhombic and rhombohedral phases. Our first-principles LAPW LDA calculations reproduced the value of Singh, and we have also calculated $V_{zz} = -2.24 \times 10^{21}$ V m^{-2} using GGA/PBE [15], which is in better agreement with experiment. The experimental rhombohedral volume and structure were

Table 2. ^{17}O NMR data in SrTi $^{16}O_{0.285}$ $^{17}O_{0.43}$ $^{18}O_{0.285}$. Chemical shift values are given relative to H_2O.

Temperature	ν_Q (MHz)	$\lvert V_{zz}\rvert$ (V m^{-2})	δ_{iso} (ppm)	δ_{ax} (ppm)	δ_{iso} [13]
150 K: cubic phase	0.1530(5)	1.622×10^{21}	467(5)	−135.3(5)	468.1
80 K: tetragonal phase	0.1521(5)	1.612×10^{21}	470(5)	−137.3(5)	—
10 K: ferroelectric phase	0.1518(5)	1.609×10^{21}	464(5)	−133.9(5)	—

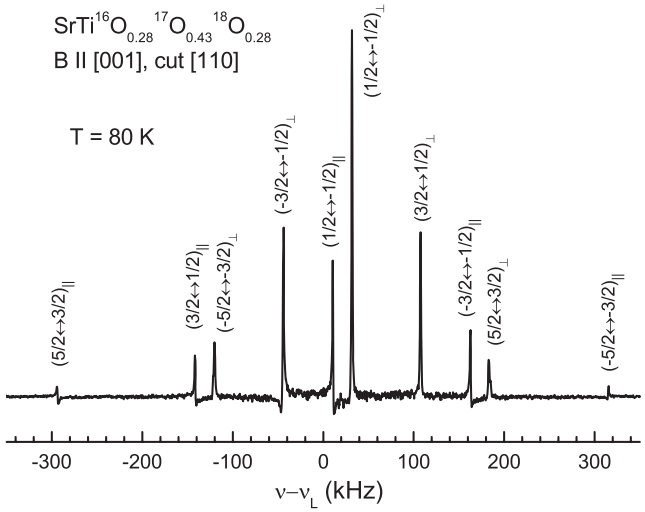

Figure 3. Quadrupole perturbed ^{17}O NMR spectrum of SrTi $[^{16}O_{0.285}$ $^{17}O_{0.43}$ $^{18}O_{0.285}]_3$ at 80 K. The indices '‖' and '⊥' denote that the magnetic field $\mathbf{B}_0$ is parallel or perpendicular to the largest principal axis of the EFG tensor at the given O sites.

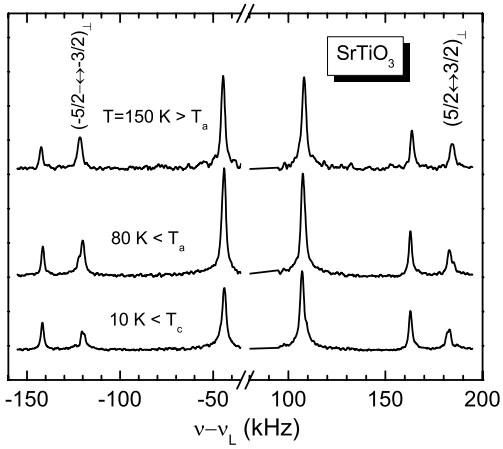

Figure 4. ^{17}O NMR spectra of SrTi $[^{16}O_{0.285}$ $^{17}O_{0.43}$ $^{18}O_{0.285}]_3$ on cooling from the cubic phase at 150 K to the tetragonal phase at 80 K and the ferroelectric phase at 10 K. Changes in lineshape are visible only for $(\pm 5/2 \leftrightarrow \pm 3/2)$ satellite transitions at $\mathbf{B}_0 \perp [001] \parallel c$.

used. For the ideal cubic phase our LDA yielded for the lattice parameter $a = 0.4004$ nm $V_{zz} = -2.35 \times 10^{21}$ V m^{-2}, in good agreement with the measured value $V_{zz} = -2.458 \times 10^{21}$ V m^{-2}.

The ^{17}O NMR spectrum of a SrTi $[^{16}O_{0.285}$ $^{17}O_{0.43}$ $^{18}O_{0.285}]_3$ single crystal with a ferroelectric transition temperature $T_c = 12$ K is shown in figure 3 for $\mathbf{B}_0 \| [001]$ at 80 K. The crystal cut is [110]. Similarly as in $BaTiO_3$ there are three physically non-equivalent but chemically equivalent ^{17}O sites in the cubic phase with local tetragonal symmetry. The largest principal axes again point along the [100], [010] and [001] directions respectively. At $\mathbf{B}_0 \| [001]$ the lines from two O sites coincide whereas the lines from the third site are displaced and weaker by a factor of two. The surprising fact is that the ^{17}O quadrupole frequency is much smaller than in $BaTiO_3$ and amounts to $\nu_Q = 153 \pm 0.5$ kHz in the cubic phase at 150 K. The corresponding quadrupole coupling constant is thus only $K = 1.016$ MHz, whereas it is 1.54 MHz in $BaTiO_3$. This is also found in our smaller first-principles calculated LDA (GGA) values of $V_{zz} = -1.0 \times 10^{21}$ V m^{-2} (-1.37×10^{21} V m^{-2}), using the experimental lattice parameter.

The changes in the ^{17}O spectra on cooling to the ferrodistortive tetragonal and ferroelectric phases are small (figure 4) and the quadrupole frequencies are practically the same as in the cubic phase (table 2). The isotropic part of the ^{17}O chemical shift tensor is 467 ppm in the cubic and 470 ppm in the tetragonal phase. The corresponding anisotropic parts are $\delta_{ax} = -135$ and -137 ppm (table 2). One should also note that the isotropic chemical shift again agrees with that reported earlier [13]. Our chemical shift anisotropy and quadrupole coupling data on the other hand differ considerably from the data derived from powder spectra [13].

The anti-parallel rotation of the oxygen octahedrons around the Ti–O–Ti axis (figure 1) on going from the cubic to the tetragonal phase at $T_a = 104$ K produces a quadrupole splitting of the $(5/2 \leftrightarrow 3/2)_\perp$ transition of $\Delta\nu \approx 0.26$ kHz (figure 4). The splitting of the $(5/2 \leftrightarrow 3/2)$ transition on going to the ferroelectric phase is also rather small. At 10 K it amounts to only 0.44 kHz. This shows that the oxygen network in $SrTiO_3$ is rather rigid and that expected shifts of Sr and Ti ions at the ferroelectric phase transition in isotopically enriched $SrTiO_3$ are very small, i.e. around 10^{-1} of those in $BaTiO_3$.

The basic result of this study is the relatively large difference between the EFG values at the oxygen sites of $BaTiO_3$ and $SrTiO_3$. Indeed the EFG in $BaTiO_3$ is surprisingly larger (about 50%) even in the cubic phase, where structural parameters of these two materials are practically identical. The lattice constant of $BaTiO_3$ ($a = 0.4009$ nm at 420 K [1]) is even a bit larger than that of $SrTiO_3$ ($a = 0.3900$ nm at 145 K [23]). Taking into account the identical crystal structure of $BaTiO_3$ and $SrTiO_3$ in the cubic phase, the above results for the EFG at the oxygen site are indeed surprising. The simple point charge model is of course not able to predict this result due to large covalency of the Ti–O bond.

On the other hand, the first-principles EFG calculations predict indeed a much smaller V_{zz}(O) value in $SrTiO_3$

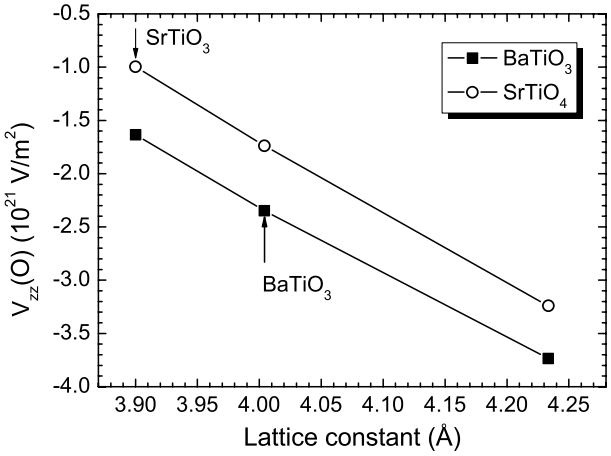

Figure 5. V_{zz}(O) as a function of lattice constant in cubic $BaTiO_3$ and $SrTiO_3$ from first-principles LAPW calculations (see text).

than in $BaTiO_3$, consistent with experimental results. EFG calculations for cubic $BaTiO_3$ and $SrTiO_3$, as a function of volume, indicate that the difference in V_{zz}(O) can be attributed to the differences in the ionic radii of the A-site cations: r_A(Ba) = 1.61 Å and r_A(Sr) = 1.44 Å [24]. The calculated volume dependences of V_{zz}(O) in cubic $BaTiO_3$ and $SrTiO_3$ (shown in figure 5) exhibit an approximately linear variation, with nearly identical slopes.

As the volume increases, the Ti–O bond length increases, allowing larger density distortions due to O(2p)–Ti(3d) hybridization and reduced short-range Ti–O ion–core repulsion. The fact that the slopes are similar reflects the same degree of O(2p)–Ti(3d) hybridization in $BaTiO_3$ and $SrTiO_3$. This is also reflected by the similar Ti and O anomalous Born effective charge tensors [9] in both crystals. For a *given* volume, however, the ionic radius of the A atom will affect the magnitude of the density distortions, with the larger Ba ion, r_A(Ba) = 1.61 Å, causing a greater distortion of the charge density near O. This results in an increase of $\sim 0.6 \times 10^{21}$ V m^{-2} in the V_{zz}(O) of $BaTiO_3$ as compared to $SrTiO_3$ (figure 5). Thus the larger r_A(Ba) leads to a larger value of $|V_{zz}(O)|$ in $BaTiO_3$ as compared to $SrTiO_3$ due to two effects. The first effect is connected with the larger equilibrium lattice constant a = 4.004 Å in $BaTiO_3$ (a = 3.900 Å in $SrTiO_3$). Figure 5 shows that this change in volume causes $|V_{zz}(O)|$ to increase by $\sim 0.7 \times 10^{21}$ V m^{-2}, for both $BaTiO_3$ and $SrTiO_3$. Second, the larger r_A(Ba) results in a V_{zz}(O) that is about 0.6×10^{21} V m^{-2} larger in $BaTiO_3$ than in $SrTiO_3$ for any given volume. Together, these two effects yield a difference of $\sim 1.3 \times 10^{21}$ V m^{-2} between cubic $BaTiO_3$ and cubic $SrTiO_3$. This is of the same order but somewhat larger than the observed value of 0.85×10^{21} V m^{-2}.

The results obtained support the importance of covalency in the onset of ferroelectricity. First-principles calculations [7, 8] have shown that ferroelectricity arises from a competition between favorable long-range ionic interactions and short-range interatomic repulsions that oppose it. At ambient pressures, covalency reduces the short-range repulsions, resulting in the ferroelectric state, while at higher pressures, i.e. smaller volume, ferroelectricity is suppressed due to the excessive energy cost of the covalent density distortions.

A special case is ferroelectricity in isotopically enriched $SrTiO_3$. Itoh *et al* discovered [11] that replacing ^{16}O by ^{18}O in $SrTiO_3$ induces a ferroelectric phase below 24 K. Ferroelectricity was also observed in the ^{16}O–^{17}O–^{18}O mixed system. It has been suggested that this surprising isotope effect is due to the fact that unenriched $SrTiO_3$ is a quantum paraelectric [25, 26], where ferroelectricity at low temperatures ($T \rightarrow 0$) is suppressed by large zero-point quantum fluctuations of the ferroelectric order parameter [26, 27]. In the ^{18}O and ^{17}O isotopically enriched samples zero-point quantum fluctuations are reduced in view of the increased average mass of the oxygen, thus allowing for the occurrence of ferroelectricity. Recent ^{87}Sr NMR measurements [28] have also shown the presence of an order–disorder component and suggested the possibility of a percolation type transition.

In conclusion, we have for the first time determined the ^{17}O EFG and chemical shift tensors in isotopically enriched $BaTiO_3$ and $SrTiO_3$ single crystals. This is the first determination of the ^{17}O EFG and chemical shift tensors in any oxide perovskite crystal. The fact that the difference between the ^{17}O chemical shift tensors in the cubic phase of $BaTiO_3$ and $SrTiO_3$ is small while the difference in the ^{17}O EFG tensors is large is generally unexpected and cannot be predicted by the point charge model. The density functional theory calculations show that this difference between $BaTiO_3$ and $SrTiO_3$ arises from the larger ionic radius of Ba versus Sr and the larger crystal cell volume of $BaTiO_3$.

Acknowledgments

Financial support from the European Union within the research network MULTICERAL no 032616 is acknowledged. HK acknowledges support from ONR grant N000140510055. Calculations were performed at the Center for Piezoelectrics by Design (CPD).

References

[1] Lines M E and Glass A M 1977 *Principles and Applications of Ferroelectrics and Related Materials* (Oxford: Clarendon)
[2] Slater J C 1950 *Phys. Rev.* **78** 748
[3] Cochran W 1960 *Adv. Phys.* **9** 387
Harada J, Axe J D and Shirane G 1971 *Phys. Rev.* B **4** 155
[4] For a recent review see, Lemanov V V 2002 *Ferroelectrics* **265** 1
[5] Bilz H, Benedek G and Bussmann-Holder A 1987 *Phys. Rev.* B **35** 4840
[6] Busmann-Holder A, Dalal N S, Fu R and Migon R 2001 *J. Phys.: Condens. Matter* **13** L231
[7] Cohen R E and Krakauer H 1990 *Phys. Rev.* B **42** 6416
[8] Cohen R E 1992 *Nature* **358** 136
[9] Zhong W, King-Smith R D and Vanderbilt D 1994 *Phys. Rev. Lett.* **72** 3618
Sommer R, Maglione R and Van der Klink J J 1990 *Ferroelectrics* **107** 307
[10] Megaw H D 1954 *Acta Crystallogr.* **7** 187
[11] Itoh M, Wang R, Inaguma Y, Yamaguchi T, Shan Y-J and Nakamura T 1999 *Phys. Rev. Lett.* **82** 3540

[12] Spearing D R and Stebbins J F 1994 *J. Am. Ceram. Soc.* **77** 3263
[13] Bastow T J, Dirken P J, Smith M E and Whitfield H J 1996 *J. Phys. Chem.* **100** 18539
[14] Hedin L and Lundqvist B I 1971 *J. Phys. C: Solid State Phys.* **4** 2064
[15] Perdew J P, Burke K and Ernzerhof M 1996 *Phys. Rev. Lett.* **77** 3865
[16] Singh D J 1994 *Planewaves, Pseudopotentials and the LAPW Method* (Boston: Kluwer Academic)
[17] Monkhorst H J and Pack J D 1976 *Phys. Rev.* B **13** 5188
[18] Abragam A 1961 *The Principles of Nuclear Magnetism* (New York: Oxford University Press)
[19] Computer program EPR-NMR, Department of Chemistry, University of Saskatchewan, Canada
[20] Singh D 1994 *Ferroelectrics* **153** 183
[21] Chaves A S, Barreto F C S, Nogueira R A and Žekš B 1976 *Phys. Rev.* B **13** 207
See also Comes R, Lambert M and Guinier A 1968 *Solid State Commun.* **6** 715
[22] Zalar B, Laguta V V and Blinc R 2003 *Phys. Rev. Lett.* **90** 037601
[23] Abramov Yu A, Tsirelson V G, Zavodnik V E, Ivanov S A and Brown I D 1995 *Acta Crystallogr.* B **51** 942
[24] Shannon R D 1976 *Acta Crystallogr.* A **32** 751
[25] Barret J H 1952 *Phys. Rev.* **86** 118
[26] Müller K A and Burkard H 1979 *Phys. Rev.* B **19** 3593
[27] Zhong W and Vanderbilt D 1996 *Phys. Rev.* B **53** 5047
[28] Blinc R, Zalar B, Laguta V V and Itoh M 2005 *Phys. Rev. Lett.* **94** 147601